Short paper

Thermal Protection of Piezoelectric Actuators Using Complex Electrical Power Measurements and Simplified Thermal Models

Yuen K. Yong, Arnfinn A. Eielsen, and Andrew J. Fleming

***Abstract*—This article describes a method for estimating the temperature of high-power piezoelectric actuators when a direct temperature measurement is impractical. The heat flow is estimated from the real component of the electrical power; then, the temperature is estimated by a transfer function that approximates the thermal response of the system. The transfer function can be derived analytically from a lumped-element approximation or calibrated experimentally by using a system identification method. The proposed method is demonstrated on a piezoelectric stack actuator used in a high-speed nanopositioning device. A second-order transfer function estimates the temperature to within 3 °C of a reference measurement for a range of operating conditions. The proposed method is suitable for protecting piezoelectric actuators in applications where direct temperature measurement is impractical, for example, due to space or wiring constraints.**

***Index Terms*—High speed, piezoelectric actuators, thermal protection.**

I. Introduction

When driven at high frequencies, piezoelectric actuators are prone to overheating due to electrical resistance, viscous damping, and dielectric and hysteresis losses [1], [2], [3]. Applications that may require high frequencies include high-speed nanopositioning [4], [5], [6], [7], [8], [9], [10], fast mirror steering systems [11], [12], ultrasonic drives [13], [14], and video-rate atomic force microscopy [15], [16]. The temperature rise induces thermal stress, which reduces the lifetime of piezoelectric ceramics [17], [18]. To prevent overheating, temperature sensors can be installed [19]; however, this may be impractical in cases where there is limited access or where the actuator is small compared to the size of the sensor.

This article describes a temperature estimation technique for the protection of piezoelectric actuators. The heat flow is estimated by measuring the real component of the electrical power. A second-order transfer function is then fitted to the power and temperature measurements to estimate the thermal response of the actuator.

In the past, thermodynamic and heat transfer models have been developed to estimate temperature rise in piezoelectric actuators [3], [20], [21], [22], [23]. However, most of these models require knowledge of the thermal properties of the piezoelectric and surrounding materials, typically the thermal conductivity, thermal diffusivity, and specific heat capacity. Data for these properties vary in the literature. The reported specific heat capacity of a piezoelectric material ranges from 350 to 491 J/kg°K at room temperature [24]. To obtain accurate thermal properties, it is often required to measure the specific heat and thermal conductivity experimentally [20]. Another approach for temperature estimation is to measure the electrical impedance over a particular frequency range [25], [26]. A disadvantage with this method is that the actuator cannot be utilized while the impedance is being measured. Also, the measured electrical impedance may be dependent on the magnitude of the input voltage, bias voltage, and mechanical stress [27]. Due to the requirement for an impedance analyzer and the associated difficulties, such methods have not been widely adopted in practice.

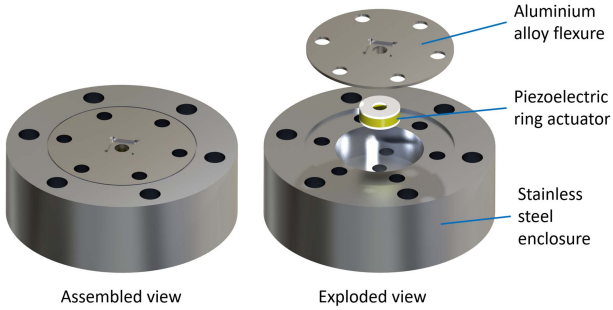

Fig. 1. High-speed nanopositioning system driven by a piezoelectric ring stack actuator.

The proposed temperature estimation technique exploits the linear relationship between the dissipated real power and the resulting temperature. Since this relationship behaves like a linear system, it can be readily determined by system identification. This approach does not require the independent measurement of thermal conductivity and specific heat capacity.

The rest of this article is organized as follows. Section II presents the derivation of the thermal model of a nanopositioning system using an equivalent thermal circuit. The model shows that the system can be represented by a linear second-order transfer function. System identification and the validation of the estimation technique are presented in Section III. Finally, Section IV concludes this article.

II. Thermal Model

This section derives the thermal model of a high-speed nanopositioning system shown in Fig. 1. A Thorlabs PA44LE piezoelectric ring actuator is used to drive the nanopositioning system at high speed. A circular flexure made of aluminum alloy Al7075 is used to preload the

Manuscript received 30 November 2022; revised 24 March 2023; accepted 28 April 2023. This work was supported by Australian Research Council. Recommended by Technical Editor G. Carbone and Senior Editor S. Katsura. *(Corresponding author: Yuen K. Yong.)*

Yuen K. Yong and Andrew J. Fleming are with the School of Engineering, University of Newcastle, Callaghan, NSW 2308, Australia (e-mail: yuenkuan.yong@newcastle.edu.au; andrew.fleming@newcastle.edu.au).

Arnfinn A. Eielsen is with the University of Stavanger, 4021 Stavanger, Norway (e-mail: eielsen@ux.uis.no).

Color versions of one or more figures in this article are available at https://doi.org/10.1109/TMECH.2023.3277437.

Digital Object Identifier 10.1109/TMECH.2023.3277437

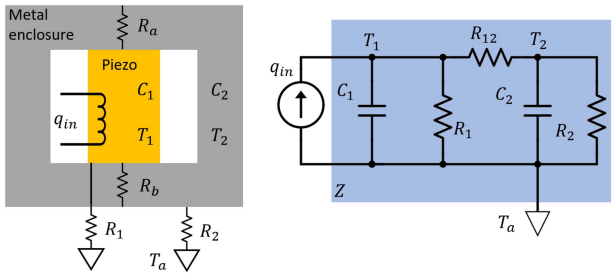

Fig. 2. Thermal model of the nanopositioner (left) and its circuit (right), where T_a is the ambient temperature.

actuator and guide the motion. The actuator is secured to a stainless steel enclosure. The nanopositioning system has the first mechanical resonance frequency at 55 kHz and a maximum stroke of 1 μm.

The thermal system and its equivalent circuit are shown in Fig. 2. The thermal resistance of the actuator, flexure, and metal enclosure is small compared with the thermal resistance to the environment [28]. The piezoelectric actuator is, therefore, modeled as a thermal mass with a uniform temperature T_1. The flexure and metal enclosure are lumped as one entity with a uniform temperature T_2. The piezoelectric actuator is modeled as a power source q_{in} (in watts), which is represented by a current source in the equivalent thermal circuit. A thermal mass C_1 represents the thermal mass of the actuator, and R_1 represents the thermal resistance between the actuator and ambient. Similarly, a thermal mass C_2 represents the enclosure, and R_2 represents the thermal resistance between the enclosure and ambient. $R_{12} = R_a||R_b$ represents the thermal resistance between the actuator and the metal enclosure. This one-dimensional simplification assumes that the temperature change along the piezo length is small compared with the absolute temperature, and that the majority of heat loss is due to conduction and convection rather than radiation. Since there is no dependence on absolute temperature, the temperatures T_1 and T_2 are defined as the rise above ambient T_a.

From the thermal circuit in Fig. 2, the Laplace transform of T_1 can be expressed as

$$T_1(s) = q_{\text{in}}(s)Z(s) \tag{1}$$

where $Z(s)$ is the input impedance of the thermal circuit. The transfer function from input $q_{\text{in}}(s)$ to output $T_1(s)$ is

$$\begin{aligned}\frac{T_1(s)}{q_{\text{in}}(s)} &= Z(s) \\ &= \left(\frac{1}{C_1 s}||R_1\right) + R_{12} + \left(\frac{1}{C_2 s}||R_2\right) \\ &= \left(\frac{R_1}{R_1C_1s+1}\right) + R_{12} + \frac{R_2}{R_2C_2s+1} \\ &= \frac{\alpha_1 s^2 + \alpha_2 s + \alpha_3}{(R_1C_1s+1)(R_2C_2s+1)}.\end{aligned} \tag{2}$$

where $\alpha_1 = (C_1C_2R_1R_2R_{12})$, $\alpha_2 = (C_1R_1R_{12} + C_1R_1R_2 + C_2R_1R_2 + C_2R_2R_{12})$, and $\alpha_3 = R_1 + R_{12} + R_2$. Equation (2) shows that the relationship between the power and the temperature can be approximated by a second-order linear transfer function with two poles and two zeros. Due to the simplicity of the model structure, linear system identification techniques can be applied to directly estimate the thermal model from experiments, which is described in the following section.

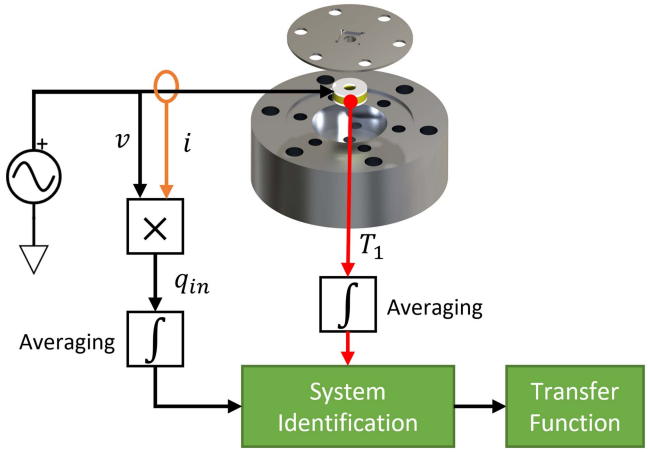

Fig. 3. Experimental setup for temperature measurement and model calibration.

III. System Identification and Model Validation

The experimental setup is shown in Fig. 3. A K-type thermocouple (TME KA02) is attached to the ring stack actuator to measure temperature. A 25-kHz sinusoidal input is generated using a signal generator (Keysight 33500B) and amplified by a PiezoDrive PD200 voltage amplifier. The drive signal amplitude is varied from 48 Vpk-pk to zero in a series of step changes over 1500 s, which results in the power dissipation plotted in Fig. 4(a). Due to the conservation of energy, the only variable that influences heat flow is the real component of electrical power applied to the piezo terminals. An identical power dissipation profile can be observed by keeping the drive amplitude constant and varying the frequency, for example.

The real power dissipation was measured every 1 s, using a Tektronix MS054 oscilloscope controlled by a MATLAB script. The oscilloscope acquires the voltage and current waveforms over 1 s, then multiplies, and averages the result to measure the average real power dissipation over 1 s, as illustrated in Fig. 3.

Using the power as an input and the measured temperature as an output, a second-order transfer function with two poles and two zeros was fitted to data using the MATLAB System Identification Toolbox. The obtained transfer function from power P_{in} (W) to temperature T_o (°C) is

$$G(s) = \frac{T_o(s)}{P_{\text{in}}(s)} = \frac{0.48229(s+1.038)(s+0.002015)}{(s+0.1062)(s+0.0009972)}. \tag{3}$$

The transfer function is further simplified by removing the fast real zero at -1.038, which has negligible effect on the system response. The simplified transfer function is

$$\tilde{G}(s) = \frac{0.50085(s+0.002015)}{(s+0.1062)(s+0.0009972)} \tag{4}$$

where the gain constant is adjusted to match the dc gain of (3).

The transfer function in (4) is validated by three independent datasets, shown in Fig. 4(c)–(h). The estimated and measured temperatures show an absolute error of less than 3 °C for a wide range of input power profiles, which validates the proposed method.

The model structure applies to a wide range of nanopositioning systems where the heat transfer can be approximated by a single dimension. However, the model parameters must be experimentally identified for each new device.

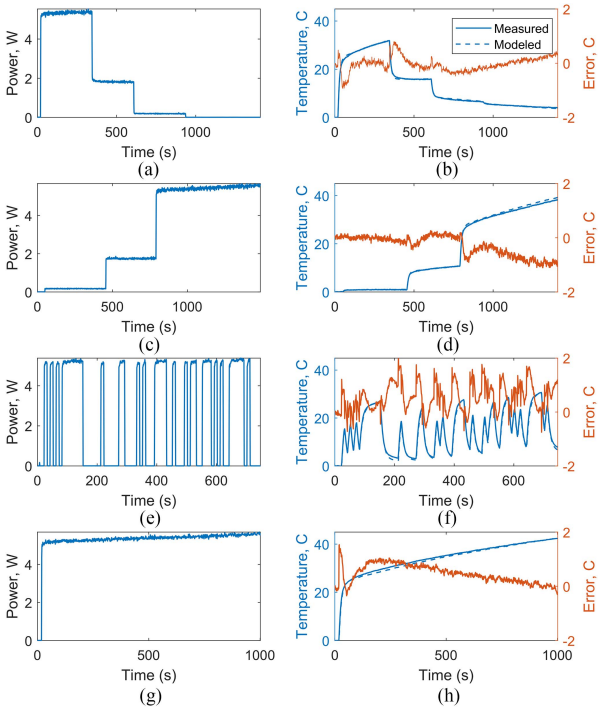

Fig. 4. Input power measurements (left column), and comparison of the measured and estimated output temperatures (right column). (a) and (b) are calibration data used to identify the model in (4). (c)–(h) are validation data used to evaluate the accuracy of the temperature estimation technique.

IV. Conclusion

The proposed method estimates the temperature of a piezoelectric actuator from the measured electrical power and a transfer function that represents the thermal dynamics of the system. This method is intended for protecting actuators against overheating when a direct temperature measurement is not feasible or desirable. Experimental results on a high-speed nanopositioning stage demonstrate that the estimated actuator temperature is within 3 °C of a reference temperature measurement. The estimation accuracy is shown to be independent of the drive amplitude and frequency and does not require knowledge of any thermal properties.

References

[1] J. Zheng, S. Takahashi, S. Yoshikawa, K. Uchino, and J. W. C. De Vries, "Heat generation in multilayer piezoelectric actuators," *J. Amer. Ceram. Soc.*, vol. 79, no. 12, pp. 3193–3198, 1996.

[2] P. Ronkanen, P. Kallio, M. Vilkko, and H. Koivo, "Self heating of piezoelectric actuators: Measurement and compensation," in *Proc. 4th Symp. Micro-Nanomechatronics Inf.-Based Soc.*, 2004, pp. 313–318.

[3] K. Yao, K. Uchino, Y. Xu, S. Dong, and L. C. Lim, "Compact piezoelectric stacked actuators for high power applications," *IEEE Trans. Ultrason., Ferroelectr., Freq. Control*, vol. 47, no. 4, pp. 819–825, Jul. 2000.

[4] X. Gao, Y. Liu, S. Zhang, J. Deng, and J. Liu, "Development of a novel flexure-based XY platform using single bending hybrid piezoelectric actuator," *IEEE/ASME Trans. Mechatronics*, vol. 27, no. 5, pp. 3977–3987, Oct. 2022.

[5] Z. Chen, J. Shi, Z. Li, X. Zhong, and X. Zhang, "A damped decoupled XY nanopositioning stage embedding graded local resonators," *IEEE/ASME Trans. Mechatronics*, vol. 27, no. 1, pp. 256–267, Feb. 2022.

[6] X. Liu et al., "Noncontact 3-D orientation control at microscale: Hydrodynamic out-of-plane rotation and in-plane rotation by compacted rotational stage," *IEEE/ASME Trans. Mechatronics*, vol. 27, no. 6, pp. 4807–4818, Dec. 2022.

[7] Y. K. Yong and A. J. Fleming, "High-speed vertical positioning stage with integrated dual-sensor arrangement," *Sens. Actuators A: Phys.*, vol. 248, pp. 184–192, 2016.

[8] Y. K. Yong, S. O. R. Moheimani, B. J. Kenton, and K. K. Leang, "Invited review article: High-speed flexure-guided nanopositioning: Mechanical design and control issues," *Rev. Sci. Instrum.*, vol. 83, no. 12, 2012, Art. no. 121101.

[9] Y. K. Yong, S. P. Wadikhaye, and A. J. Fleming, "High-speed single-stage and dual-stage vertical positioners," *Rev. Sci. Instrum.*, vol. 87, 2016, Art. no. 085104.

[10] Y. K. Yong and S. O. R. Moheimani, "A compact XYZ scanner for fast atomic force microscopy in constant force contact mode," in *Proc. IEEE/ASME Int. Conf. Adv. Intell. Mechatronics*, 2010, pp. 225–230.

[11] E. Csencsics, B. Sitz, and G. Schitter, "Integration of control design and system operation of a high performance piezo-actuated fast steering mirror," *IEEE/ASME Trans. Mechatronics*, vol. 25, no. 1, pp. 239–247, Feb. 2020.

[12] E. Csencsics and G. Schitter, "Exploring the pareto fronts of actuation technologies for high performance mechatronic systems," *IEEE/ASME Trans. Mechatronics*, vol. 26, no. 2, pp. 1053–1063, Apr. 2021.

[13] B. Zhu, W. Wei, X. Yang, Y. Li, Q. Zhou, and K. K. Shung, "KNN-based single crystal high frequency transducer for intravascular photoacoustic imaging," in *Proc. IEEE Int. Ultrason. Symp.*, 2017, pp. 1–1.

[14] R. Chen et al., "Eco-friendly highly sensitive transducers based on a new KNN–NTK–FM lead-free piezoelectric ceramic for high-frequency biomedical ultrasonic imaging applications," *IEEE Trans. Biomed. Eng.*, vol. 66, no. 6, pp. 1580–1587, Jun. 2019.

[15] T. Ando, "High-speed atomic force microscopy coming of age," *Nanotechnology*, vol. 23, no. 6, 2012, Art. no. 062001.

[16] Y. K. Yong, A. Bazaei, and S. O. R. Moheimani, "Video-rate Lissajous-scan atomic force microscopy," *IEEE Trans. Nanotechnol.*, vol. 13, no. 1, pp. 85–93, Jan. 2014.

[17] X. Lu and S. V. Hanagud, "Extended irreversible thermodynamics modeling for self-heating and dissipation in piezoelectric ceramics," *IEEE Trans. Ultrason., Ferroelectr., Freq. Control*, vol. 51, no. 12, pp. 1582–1592, Dec. 2004.

[18] O. Drozdenko, K. Drozdenko, and L. Perchevska, "Methods for analyzing the thermal field of rod type piezoceramic electroacoustic transducer," in *Proc. IEEE 39th Int. Conf. Electron. Nanotechnol.*, 2019, pp. 750–753.

[19] W.-S. Ohm, J. H. Kim, and E. C. Kim, "Prediction of surface temperature rise of ultrasonic diagnostic array transducers," *IEEE Trans. Ultrason., Ferroelectr., Freq. Control*, vol. 55, no. 1, pp. 125–138, Jan. 2008.

[20] H. N. Shekhani and K. Uchino, "Characterization of mechanical loss in piezoelectric materials using temperature and vibration measurements," *J. Amer. Ceram. Soc.*, vol. 97, no. 9, pp. 2810–2814, 2014.

[21] J. Hu, "Analyses of the temperature field in a bar-shaped piezoelectric transformer operating in longitudinal vibration mode," *IEEE Trans. Ultrason., Ferroelectr., Freq. Control*, vol. 50, no. 6, pp. 594–600, Jun. 2003.

[22] Y. Li, X. Shen, X. Kou, and L. Yu, "Design, experiment, and verification of a heating and insulation structure for the piezoelectric stack," *J. Intell. Mater. Syst. Struct.*, vol. 31, no. 5, pp. 719–736, 2020.

[23] S.-W Zhou and C. A. Rogers, "Heat generation, temperature, and thermal stress of structurally integrated piezo-actuators," *J. Intell. Mater. Syst. Struct.*, vol. 6, no. 3, pp. 372–379, 1995.

[24] M. Stewart and M. G. Cain, "Measurement and modelling of self-heating in piezoelectric materials and devices," in *Characterisation of Ferroelectric Bulk Materials and Thin Films* (Springer Series in Measurement Science and Technology), vol. 2, M. G. Cain, Ed. Dordrecht, The Netherlands: Springer, 2014, pp. 147–189.

[25] J. Ilg, S. J. Rupitsch, and R. Lerch, "Impedance-based temperature sensing with piezoceramic devices," *IEEE Sens. J.*, vol. 13, no. 6, pp. 2442–2449, Jun. 2013.

[26] S. J. Rupitsch, J. Ilg, and R. Lerch, "Inverse scheme to identify the temperature dependence of electromechanical coupling factors for piezoceramics," in *Proc. Joint IEEE Int. Symp. Appl. Ferroelectr. Workshop Piezoresponse Force Microsc.*, 2013, pp. 183–186.

[27] J. B. Liseli, J. Agnus, P. Lutz, and M. Rakotondrabe, "Self-sensing method considering the dynamic impedance of piezoelectric based actuators for ultralow frequency," *IEEE Robot. Autom. Lett.*, vol. 3, no. 2, pp. 1049–1055, Apr. 2018.

[28] J. Wojtkowiak, "Lumped thermal capacity model," in *Encyclopedia of Thermal Stresses*, R. B. Hetnarski, Ed. Dordrecht, The Netherlands: Springer, 2014, pp. 2808–2817.